

Scanning Two-Photon Fluctuation Correlation Spectroscopy: Particle Counting Measurements for Detection of Molecular Aggregation

K. M. Berland, P. T. C. So, Y. Chen, W. W. Mantulin, and E. Gratton

Laboratory for Fluorescence Dynamics, Department of Physics, University of Illinois at Urbana-Champaign, Urbana, Illinois 61801 USA

ABSTRACT Scanning fluctuation correlation spectroscopy (FCS) is an experimental technique capable of measuring particle number concentrations by monitoring spontaneous equilibrium fluctuations in the local concentration of a fluorescent species in a small (femtoliter) subvolume of a sample. The method can be used to detect molecular aggregation for dilute, submicromolar samples by directly "counting particles." We introduce the application of two-photon excitation to scanning FCS and discuss its important advantages for this technique. We demonstrate the capability of measuring particle number concentrations in solution, first with dilute samples of monodisperse 7-nm and 15-nm radius latex spheres, and then with B phycoerythrin. The detection of multiple species in a single sample is shown, using mixtures containing both sphere sizes. The method is then applied to study protein aggregation in solution. We monitor the concentration-dependent association/dissociation equilibrium for glycogen phosphorylase A and malate dehydrogenase. The measured dissociation constants, 430 nM and 144 nM respectively, are in good agreement with previously published values. In addition, oligomer dissociation induced by pH titration from pH 8 to pH 5.0 is detectable for the enzyme phosphofructokinase. The possibility of measuring dissociation kinetics by scanning two-photon FCS is also demonstrated using phosphofructokinase.

INTRODUCTION

In this paper we investigate the particle-counting capability of two-photon scanning fluctuation correlation spectroscopy (FCS) to detect the association of biomolecules in solution. The method is used to measure number concentrations over many orders of magnitude of dilute concentration ($<10 \mu\text{M}$). The high sensitivity and selectivity of fluorescence measurements and the strong background rejection of two-photon excitation are exploited for low background counting of particles in the excited volume. The particle detection limits are determined by the fluorescence intensity from individual molecules rather than particle size, and the instrument is able to detect single molecules. The statistics of the particle counting and the detection of aggregation are analyzed based on autocorrelation of the measured fluorescence. The measured autocorrelation contains information on both particle number concentration and particle mobility. Here we consider only the measurements of number concentrations. We have previously evaluated the instrument performance for measuring diffusion coefficients in solution and in live cells (Berland et al., 1995). Other applications using correlation analysis to measure the mobility with single-particle sensitivity have been described (Eigen and Rigler, 1994; Mets and Rigler, 1994; Widengren et al.,

1994) and include the detection of interactions in solution based on altered mobility (Rigler et al., 1992).

In a typical FCS experiment (Elson and Magde, 1974; Elson et al., 1974; Magde et al., 1974; see Thompson, 1991, for a review), fluorescence intensity from a subvolume of a sample serves as a measure of the number of particles in an excited volume. Spontaneous equilibrium fluctuations will cause this occupation number to vary about the average value, both temporally and spatially, due to Brownian diffusion. For random diffusion, the fluctuations follow Poisson statistics, with an average magnitude of $N^{1/2}$ when the average occupation number is N . By comparing the average magnitude of the fluctuations with the average occupation number, the number of particles in the volume can be determined without directly calibrating how fluorescence intensity scales with number of particles. Formally, calculating the autocorrelation of the measured fluorescence intensity yields particle concentrations, as well as particle mobility.

There are two particularly important and unique advantages of applying two-photon excitation (Denk et al., 1990) to scanning FCS. The first is the inherent selection of a subvolume in a bulk sample (as in confocal) due to the quadratic dependence on excitation power of the two-photon process. This optical sectioning defines a subvolume of the sample and allows measurements to be made in bulk solution without the need for confocal pinholes, which can greatly reduce fluorescence detection efficiencies. The second advantage is the reduced background detection of laser scatter compared with one-photon excitation. When two-photon excitation is used, the fluorescence emission does not spectrally overlap with the Raman and Rayleigh scattering and can be separated by several hundred nanometers. For example, 976-nm light is used to excite the 488-nm transition of fluorescein. By choosing appropriate filters and

Received for publication 8 March 1996 and in final form 11 April 1996.

Address reprint requests to Professor Enrico Gratton, Department of Physics, University of Illinois at Urbana-Champaign, Urbana, IL 61801. Tel.: 217-244-5620; Fax: 217-244-7187.

Dr. Berland's present address is Department of Cell Biology and Anatomy, CB 7090, Taylor Hall, University of North Carolina-Chapel Hill, Chapel Hill, NC 27599. Tel.: 919-966-3855; Fax: 919-966-1856; E-mail: berland@med.unc.edu.

© 1996 by the Biophysical Society

0006-3495/96/07/410/11 \$2.00

photodetectors, one can nearly eliminate detection of scatter while maintaining high collection efficiency for the fluorescence emission. In addition, this technique has little or no background fluorescence from lenses, optics, dust, or immersion oil because the laser intensity is insufficient for two-photon excitation everywhere except at the focal volume. Low background detection is very important for counting using correlation, because any light not specific to the molecules under investigation will distort the comparison of the average fluctuation amplitudes and the average intensity.

The functional form of the measured autocorrelation function, $G(\tau)$, depends on the volume shape and has been thoroughly characterized elsewhere (Elson and Magde, 1974; Elson et al., 1974; Magde et al., 1974; Thompson, 1991; Rigler et al., 1993; Berland et al., 1995). The time 0 value of the measured fluorescence autocorrelation, $G(0)$, is related to the number concentration (number of independently diffusing particles) by (Thompson, 1991)

$$G(0) = \gamma \sum_i \frac{\alpha_i^2 \langle N_i \rangle}{\left(\sum_j \alpha_j \langle N_j \rangle \right)^2}. \quad (1)$$

The constants α_i and $\langle N_i \rangle$ are the relative fluorescence intensities and average number occupation of each species in the volume, and γ is a geometric factor dependent on the shape of the volume. For the Gaussian-Lorentzian intensity distribution used to fit the data (Berland et al., 1995), $\gamma = 0.076$. For a single species, the above equation reduces to γ/N ; i.e., the number of particles in the volume is proportional to $G(0)^{-1}$. The volume in our instrument is ~ 0.1 fl, which corresponds to an average of 0.6 particles in the volume for a 10 nM sample.

One can detect particle aggregation by comparing the number occupations measured by FCS with the number of particles expected for a known sample concentration (mg/ml). A convenient way to make this comparison is to introduce an association parameter, β :

$$\beta \equiv \frac{\gamma}{G(0) \cdot N_T}, \quad (2)$$

where N_T is the total number of monomer units (or smallest subunits) in the volume, calculated from the concentration, C , and the excited sample volume. For monodisperse samples, β will have the value $1/n$, where n is the number of monomers per particle. For a monomer-dimer equilibrium where the particle intensity scales linearly with the number of monomers, β has the form

$$\beta = \left(2 + \frac{k}{4 \cdot C} \cdot (1 - \sqrt{1 + 8C/k}) \right)^{-1}, \quad (3)$$

where k is the dissociation constant. This was derived using Eqs. 1 and 2, along with the definition of k . The same form would apply for a dimer-tetramer equilibrium with a constant prefactor, and similar formulas are easily produced for

other equilibria, such as monomer-tetramer. Fig. 1 shows β plotted for several values of k , assuming a monomer-dimer equilibrium.

The application of two-photon scanning FCS to the study of molecular aggregation is a powerful biophysical/biochemical diagnostic technique, particularly for measurements at low concentrations. The most common available experimental techniques capable of measuring the degree of association include light scattering, ultracentrifugation, electrophoresis, and fluorescence depolarization. Each of these techniques has a limited range of molecular sizes and solution concentrations where it is most effective. These methods generally work best for relatively high concentrations ($> \mu\text{M}$) and with larger molecules. The submicromolar "most effective" range of FCS complements other methods well. In addition, the high sensitivity of fluorescence relative to scattering and absorption is an important advantage. The method can be applied to study many types of protein interactions, including the subunit composition of protein oligomers and binding of enzymes to their substrates. The applications can also involve other biomolecules such as nucleic acids, ligands, or membrane receptors. In combining FCS measurements of aggregation with functional assays, it is possible to investigate how molecular interactions relate to biological function.

The results presented in this article demonstrate several particle-counting applications of our two-photon scanning FCS instrument. We demonstrate accurate counting resolution for multiple concentrations of both 7-nm- and 15-nm-radius latex spheres. The possibility of detecting and identifying the composition of samples containing multiple species is demonstrated by using mixtures of the two sizes of spheres. We then show applications of the technique to

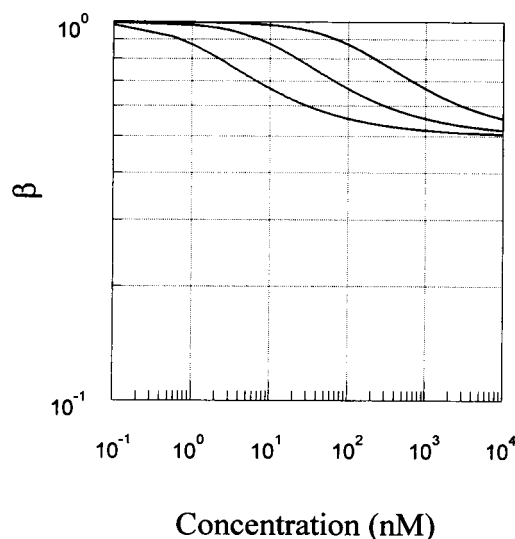


FIGURE 1 Simulations of the parameter β for a monomer dimer equilibrium. The curves shown have values for the dissociation constants of 10, 100, and 1000 nM. When plotted on the log scale, the curve crosses the point halfway between the extreme values at the concentration corresponding to the dissociation constant.

several oligomeric proteins in solution. Several concentrations of B phycoerythrin are shown as a control, and association/dissociation equilibrium is monitored for the enzymes glycogen phosphorylase A (GPA), malate dehydrogenase (MDH), and phosphofructokinase (PFK). GPA is a 390-kDa tetramer known to dissociate into dimers upon dilution. MDH is a 70-kDa dimer that dissociates into monomers, also with dilution. Both proteins are relatively well characterized and were chosen to demonstrate the potential of the instrument. The dissociation of PFK with dilution was used to demonstrate the feasibility of using scanning FCS for kinetic measurements. Furthermore, as an alternative to dilution experiments, we show the dissociation of PFK as a function of pH.

EXPERIMENTAL CONSIDERATIONS

Ideally, $G(0)$ could be directly measured experimentally (without scanning), but shot noise introduces considerable error to the first few autocorrelation channels, causing the measurement to be rather inaccurate. The simplest solution to this problem is to calculate $G(0)$ by extrapolation to zero time after fitting the measured $G(\tau)$ to an appropriate model. This method has had some success in measuring particle number concentrations (Icenogle and Elson, 1983; Palmer and Thompson, 1987, 1989b).

Scanning the beam across the sample (or the sample through the beam), known as scanning FCS, can further improve the measurement resolution. All results presented in this work use the scanning approach. Scanning FCS takes advantage of the equivalence of spatial and temporal averaging for ergodic samples. Typically, the beam is scanned periodically (with period T) in some pattern across the sample. The occupation numbers measured at varying times reflect the local particle concentrations of multiple independent sample volumes. The measured scanning autocorrelation function, $G_s(\tau)$, is periodic with peaks separated by the scan period, T (see Theory).

Scanning FCS was originally used to measure molecular weights of DNA labeled with ethidium bromide (Weissman et al., 1976). Several variations of scanning FCS with slow diffusion have been reported (Petersen, 1984, 1986; Petersen et al., 1986; St-Pierre and Petersen, 1990), as have recent imaging applications of correlation spectroscopy (Petersen et al., 1993; Huang and Thompson, 1996). Other reports have demonstrated the potential to measure diffusion coefficients and particle count simultaneously (Meyer and Schindler, 1988; Koppel et al., 1994).

The major motivation for scanning is that the signal-to-noise ratio for a given data acquisition time is greatly improved by monitoring multiple independent regions of the sample during times that no new information would be gained by continuously sampling any one subvolume. In effect, one simultaneously measures $G(\tau)$ for a large number of independent volumes. Under many experimental conditions, there is essentially no penalty for scanning, because

the time needed to measure the fluorescence from any single volume is short compared with the diffusion "turnover time," the time scale for which the particle occupation number will change due to diffusion. The turnover time depends on the ratio of the diffusion coefficient, D , and the beam waist, w_0 , ($\sim w_0^2/D$). The turnover time is in the millisecond range for diffusion coefficients of $\sim 10^{-7} \text{ cm}^2 \text{ s}^{-1}$ and a beam waist of $0.5 \text{ } \mu\text{m}$.

The resolution and accuracy of scanning FCS are determined by the experimental ability to accurately count the number of particles in the excited volume. The number of photons one can collect from each single particle in the volume, compared with all other "background" signals, is the most crucial parameter that determines the success of a correlation analysis (Koppel, 1974). The ability to recover accurate quantitative information is thus greatly aided when light collection and detection efficiencies are high and hindered by any sources of detected light other than fluorescence from the particles of interest. Clean samples and low noise detectors can eliminate much of this background. Scattered laser light, however, can cause a major noise problem. It is often impossible to prevent detecting scatter, particularly Raman scattering that spectrally overlaps with fluorescence emission. Thus, as mentioned above, two-photon excitation is particularly well suited for FCS (and other single-molecule detection studies) because it greatly reduces the detection of scattered light (Mertz et al., 1995; Berland et al., 1996; Ragan et al., 1996).

THEORY

For standard FCS measurements, the autocorrelation, $G(\tau)$, of the fluorescence intensity, $F(t)$, is defined as

$$G(\tau) = \frac{\langle F(t)F(t+\tau) \rangle}{\langle F \rangle^2} - 1 = \frac{\langle \delta F(t)\delta F(t+\tau) \rangle}{\langle F \rangle^2}. \quad (4)$$

The angle brackets represent a time average. After writing the fluorescence intensity in terms of the sample concentration, $C(\vec{r}, t)$, and the laser intensity, $I(\vec{r})$, $G(\tau)$ has the form

$$G(\tau) = \frac{\langle \int d\vec{r} d\vec{r}' I^2(\vec{r})I^2(\vec{r}') \delta C(\vec{r}, t+\tau) \delta C(\vec{r}', t) \rangle}{\langle F \rangle^2}. \quad (5)$$

The functional form of $G(\tau)$ for translational diffusion in solution has previously been reported for 3D Gaussian (Rigler et al., 1993) and Gaussian-Lorentzian (Berland et al., 1995) focused laser intensity distributions. We have found that the Gaussian-Lorentzian distribution fits the data more consistently.

The major change introduced by scanning the beam is that we must evaluate the effect on $G(\tau)$ (renamed $G_s(\tau)$) of scanning the beam $I(\vec{r}) = I(\vec{r}(t), t)$, or scanning the sample $C(\vec{r}) = C(\vec{r}(t), t)$. For these experiments, the beam is scanned in a circle. We will describe the beam scan (sample motion) with a two-dimensional periodic "scan vector," \vec{r}_s , which

specifies the beam (sample) displacement from an arbitrary rest position as a function of time:

$$\vec{r}_s = A \cos(\omega t) \hat{i} + B \sin(\omega t) \hat{j}, \quad (6)$$

where \hat{i} and \hat{j} are the unit vectors in the radial directions, and the scan period $T = 2\pi/\omega$. Assuming the beam is scanned, Eq. 5 can be rewritten as

$$G_s(\tau) = \frac{\langle \int d\vec{r} d\vec{r}' \hat{r}(\vec{r} - \vec{r}_s(t + \tau)) \hat{r}'(\vec{r}' - \vec{r}_s(t)) \delta C(\vec{r}, t + \tau) \delta C(\vec{r}', t) \rangle}{\langle F \rangle^2}. \quad (7)$$

A simple change of variables results in the following equivalent form:

$$G_s(\tau) = \frac{\langle \int d\vec{r} d\vec{r}' \hat{r}(\vec{r}) \hat{r}'(\vec{r}') \delta C(\vec{r} - \vec{r}_s(t + \tau), t + \tau) \delta C(\vec{r}' - \vec{r}_s(t), t) \rangle}{\langle F \rangle^2}, \quad (8)$$

which could have been written down directly as the form when the sample is scanned, demonstrating the theoretical equivalence of either method. In the second form, the laser intensity has no time dependence and can be evaluated outside of the time average. It can be shown for both the 3D Gaussian and Gaussian-Lorentzian models (of the focused laser intensity distribution) that the scanning form of the autocorrelation, $G_s(\tau)$, has the same form as without scanning, $G(\tau)$, but is multiplied by the following new scan factor:

$$S(t, \tau) = \exp\left(\frac{-2|\vec{r}_s(t + \tau) - \vec{r}_s(t)|^2}{(1 + (8D\tau/w_0^2))w_0^2}\right), \quad (9)$$

which, for scanning in a circle of radius A , reduces to the time-independent form:

$$S(\tau) = \exp\left(\frac{-4A^2(1 - \cos(\omega\tau))}{(1 + (8D\tau/w_0^2))w_0^2}\right). \quad (10)$$

For other scan shapes, the scan vector is not time independent, and more averaging is involved in the final form of measured autocorrelation. However, for reasonably circular shapes Eq. 10 will be a good approximation.

Thus, overall, the decay in the autocorrelation with τ is unchanged, but the entire function is modulated by the scan envelope, $S(\tau)$, of Eq. 10. Fig. 2 A demonstrates the form of the scan function simulated using typical parameters. Fig. 2 B shows a simulation of the combined form of the autocorrelation function $G_s(\tau) = S(\tau) \times G(\tau)$. The width of each peak is related to the diffusion coefficient, the beam waist, the scan radius, and the scanning rate. Theoretically, peak widths can be fit to determine the diffusion coefficient if the beam waist and scan radius are known (Meyer and Schindler, 1988). However, the finite time bins used in the measurement of the autocorrelation (see below) introduce a broadening that is not accounted for in the above theory. We are preparing a separate analysis of this effect to introduce the necessary corrections to the theory.

The peak amplitudes, $G_s(nT)$ (integer n), in the measured $G_s(\tau)$ are analyzed to determine particle concentrations. These peaks are sufficiently far from the time 0 channel to be free of the extensive noise in the first few correlation

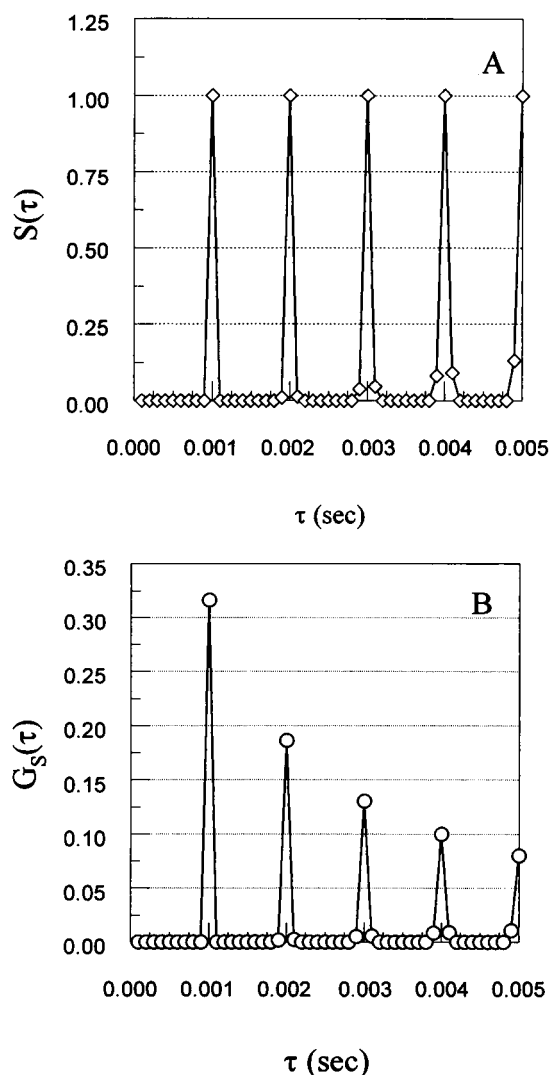


FIGURE 2 (A) Simulation of the scan factor, $S(\tau)$, shown for $D = 8 \times 10^{-7}$ cm²/s, beam waist $w_0 = 0.5$ μ m, and scan radius $A = 3$ μ m. (B) Simulation of $G_s(\tau)$, the functional form of the measured autocorrelation for scanning FCS, using the Gaussian-Lorentzian model. The parameters D , w_0 , and A are the same as in A.

channels. The scanning period, $T = 2\pi/\omega$, relative to the diffusion turnover time discussed above, will determine whether the peaks are relatively flat (slow diffusion) or decay because of faster diffusion. For slow time scales, measurements of peak amplitudes correspond directly to $G_s(0)$ and thus to $\langle N \rangle$, as in the results of Weissman et al. (1976). For faster diffusion time scales (or slower scanning), there is a decay of $G_s(nT)$ due to diffusion.

MATERIALS AND METHODS

Instruments

The two-photon FCS instrument was previously described elsewhere (Berland et al., 1995). The scanning instrument includes galvomotor-driven scanning mirrors (series 603X; Cambridge Instruments, Watertown, MA), located at the eye point of a scan lens focused at the field aperture of the

microscope tube lens. There is also a descanning lens before the photomultiplier. The scanning and descanning lenses are 10× microscope eyepieces from Zeiss (Thornwood, NY). The scanner is driven by two phase locked Hewlett Packard (Santa Clara, CA) 3325 frequency synthesizers, 90°C out of phase, scanning a circular pattern across the sample. One- and two-kilohertz scan rates were used, the latter for samples with faster diffusing particles. The scan radius, A , was typically chosen to be between 3 and 5 μm . The Coherent MIRA Ti:Sapphire (Palo Alto, CA) was set at 960 nm (80-MHz pulse rate, 150-fs pulse width). Power at the sample was 10–20 mW. Emission filters were BG39 Schott glass. Fluorescence was detected by either a Hamamatsu R5600-P (TO8) or a R1104 photomultiplier tube. The R5600 is the preferred choice, because of its very low dark noise and high quantum efficiency. Average dark counts with this tube were 6 counts/s at room temperature. Furthermore, the IR sensitivity of the R5600 is several orders of magnitude below the sensitivity in the visible range of the spectrum, further reducing the detection of scattered light. The signal from the photomultiplier was amplified and discriminated in a Pacific AD6 discriminator (Concord, CA).

To process the data, photon counts from the discriminator were divided into time bins of width Δt , $F(n\Delta t)$, by a home-built data acquisition card operating in a 486 PC. The series of time bins is transferred to the computer memory, where fluorescence correlation functions are calculated in software using the following algorithm:

$$\langle F(t)F(t + \tau_m) \rangle = \sum_{n=1}^P F(n\Delta t) \times F(n\Delta t + m\Delta t). \quad (11)$$

This quantity is normalized as in Eq. 4 to get the autocorrelation function, $G_s(\tau)$. The summation is done for M independent channels (values of τ_m), with $\tau_m = m\Delta t$ ($1 \leq m \leq M$). P is the total number of time intervals sampled, chosen to achieve a sufficient signal-to-noise ratio for analysis.

To perform a measurement, one must choose an appropriate width for the time bin, Δt . For maximum resolution, one would simply choose a time bin size that is much smaller than the diffusion turnover time mentioned above and fast compared with the scan rate. However, because the signal-to-noise ratio for the measurement depends on the number of counts detected per time bin per chromophore (Koppel, 1974), it is helpful to keep the bin size relatively large. In these measurements, the correlator time bins were 0.1 and 0.05 ms (10-, 20-kHz binning clock) for the 1- and 2-kHz scans, respectively. As mentioned above, this choice of relatively long time bins introduces a broadening of the correlated peaks. To avoid aliasing, the binning clock rate was a multiple of the scan rate.

Sample preparation

Latex spheres and phycoerythrin were purchased from Molecular Probes (Eugene, OR). Spheres were sonicated for approximately 10 min and then filtered using 0.2 μm syringe filters before diluting to the measured concentrations. B phycoerythrin was prepared according to the protocol provided and dialyzed with several changes of 50 mM phosphate-buffered saline (pH 7.5) before samples were diluted to the measured concentrations.

GPA was purchased from Sigma (St. Louis, MO). The protein was dialyzed over 24 h with four buffer changes to remove salts (50 mM Tris, 1 mM EDTA, dithiothreitol, pH 9). Fluorescein isothiocyanate (FITC) labeling was achieved by incubation overnight at 4°C with a 20 molar excess of FITC purchased from Molecular Probes. Free dye was removed on G25 Sephadex columns, and samples were subsequently filtered using 0.2- μm syringe filters. Concentrations were determined using absorption at 280 nm ($1.24 \times 10^5/(\text{M cm})$; Huang and Graves, 1970). The final labeling ratio was ~2 FITC per monomer. Dilutions were then prepared for a series of protein concentrations and allowed to sit for at least 3 h at 4°C before measurements were made.

MDH was from U.S. Biochemical Corp. (Cleveland, OH) and was labeled using the same procedure as for the GPA (50 mM Tris, pH 8). Concentration was again determined by absorption at 280 nm (17000/(M cm); D. Jameson, personal communication). After running through the G25

column, samples were dialyzed overnight to further remove free dye. Final labeling was also approximately 2 FITC per monomer.

PFK was purchased from Sigma. The crystalline protein suspension was centrifuged, and the precipitate dissolved in 0.2 M sodium bicarbonate buffer at pH 9 to a final protein concentration of 6 mg/ml. PFK was labeled with BODIPY, because FITC fluorescence is strongly pH dependent and fluorescein has low quantum efficiency at low pH. BODIPY amine labeling kits (B-2185) were from Molecular Probes, and the supplied labeling procedure was followed. Labeled protein was loaded on a G25 column, and the first colored band was collected and dialyzed against 0.1 M dipotassium phosphate buffer (1 mM EDTA, pH 7.5). The final stock concentration was 0.318 mg/ml, determined from the 280 nm absorbance using an extinction coefficient of 1.02 ml/(mg cm) (Pavelich and Hammes, 1973). Each monomer was labeled on average with 2.3 BODIPY.

Most samples were mounted on hanging drop microscope slides for scanning FCS measurements. Slides were washed and then soaked in nitric acid before each use. For some of the dilution experiments, samples were held in a small chamber on the microscope, where they were diluted and allowed to equilibrate before each measurement. Sample preparation is extremely critical for these measurements, as in all FCS techniques. Contaminants and fluorescent dust in the sample can result in substantial error.

Calibration and data analysis

What one actually measures in a scanning FCS experiment is a fluctuation size, which depends on the number of particles in the excited volume (γ/N). If the experimental interest is to measure relative changes and trends in N as an experimental parameter is varied (sample concentration, for example), no calibration is necessary. To recover an absolute particle number concentration from the measured $G_s(0)$ values, it is necessary to calibrate the size of the excited volume. This volume can in theory be calculated from the numerical aperture of the lens and the wavelength of light. However, experimental tests have generally shown "factor of 2" deviations from theoretically predicted calibrations (Palmer and Thompson, 1989b; Thompson, 1991). The calibration is also affected by the binning clock speed relative to the scan rate, which causes the peaks to broaden as mentioned above. Problems with calculated calibration can be avoided by calibrating experimentally.

Experimental calibration simply involves measuring $G_s(0)$ for a probe of known concentration and then calculating the volume from the measured $G_s(0)$ and the geometric factor γ , using Eq. 1. Our instrument was calibrated using the 7-nm-radius latex spheres. The volume obtained was 0.1 μm^3 , varying by as much as a factor of 2 any time the instrument optics were realigned. The value remained constant as long as no adjustments were made to the optical alignment. The range of volumes obtained with different alignments agrees reasonably well with theoretical calculations. The measured volume corresponds to a beam waist of 0.42 μm .

For all of the studies discussed below, measurements involved relative changes after varying sample concentration or buffer pH. The calibration was thus not critical for any of the reported results. For the sphere samples, the volume was calibrated using the above procedure. For the protein samples, we have considered only relative changes in particle associations. We have not attempted to use the absolute calibration to directly identify the number of subunits per particle, although in principle this can be done.

In the results presented here, the measured values of $G_s(T)$ are used directly to compare particle number occupations. For monodisperse samples, $G_s(T)$ differs from $G_s(0)$ by a constant factor for all sample concentrations. For samples with multiple particle sizes, the factor is not constant. With the diffusion rates considered in this work, this correction can be as much as 10–15% for particles whose molecular weights differ by a factor of 2. Future work can correct for this by fitting the whole series of peaks (or a single peak width) to correct for diffusion.

RESULTS

We first demonstrate the accuracy of this technique for particle counting by comparing the average concentration

measured by scanning FCS with the known value for several concentrations of latex spheres. Fig. 3 shows a typical measurement of $G_S(\tau)$ for 7-nm-radius latex beads in water at room temperature. Fig. 4 shows the results from a series of measurements using several concentrations of the two (7- and 15-nm radius) sphere sizes. The measured particle concentration for these spheres is generally accurate to within a few percent. These spheres are significantly smaller (and dimmer) than those used in testing the performance of other scanning FCS instruments. The ability to accurately count these smaller sphere sizes is an important test of how well an instrument will perform on biomolecules, or other particles labeled with relatively few probes. The 7-nm-radius spheres are comparable in size to many relatively large proteins, although even these smaller spheres are heavily labeled and have fluorescence intensity equivalent to many (5–10) fluorescein dyes per sphere.

Similar measurements were made using B phycoerythrin. The results are shown in Fig. 5, which plots the quantity β as a function of protein concentration. A value of 1 corresponds to nondissociated/nonaggregated B phycoerythrin. This protein does not dissociate as it is diluted over the measured concentration range, as shown. The B phycoerythrin is not as bright per particle as the spheres, and the noise is greater, although the signal-to-noise ratio remains quite good.

Ultimately, the true test of whether the method is useful for detecting macromolecular aggregation is in the ability to detect particles of multiple sizes and fluorescence intensities in a single sample. We have measured $G_S(T)$ for four separate mixtures with known concentrations of 7- and 15-nm spheres; the results are shown in Fig. 6. The measured values are plotted against the values calculated using the known concentrations. If one assumes that only two sphere sizes are present, and the relative fluorescence intensities are known, then the measured $G_S(T)$ value and the average fluorescence intensity are sufficient to calculate the composition of each sample uniquely. This result demonstrates the promise of scanning FCS for detecting the pres-

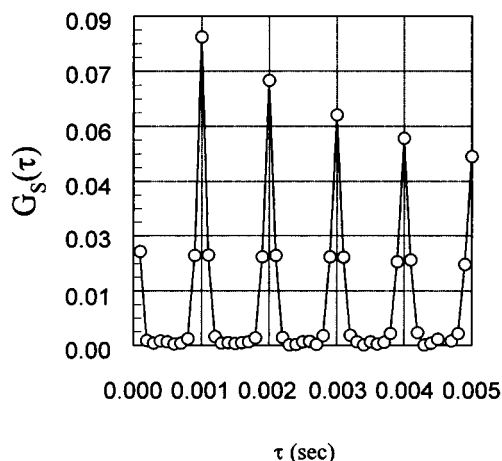


FIGURE 3 Typical measurement of $G_S(\tau)$ for 7-nm spheres in water.

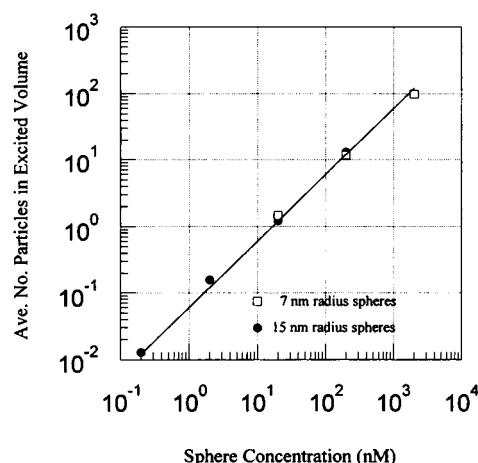


FIGURE 4 Results from measurements of $G_S(\tau)$ for a series of 7-nm and 15-nm sphere concentrations.

ence of multiple species and aggregation. If more than two species are present, one needs an additional measured parameter for each new species to recover the distribution of particles in the sample. Much work has been done on the theory of high-order correlation analysis as a method of distinguishing a broader distribution of species (Palmer and Thompson, 1987, 1989a; Qian and Elson, 1990a,b). This method has not been applied in these studies but is an additional technique available for future attempts at characterizing more complicated particle size distributions.

Protein aggregation

GPA, a 390-kDa tetramer, has been shown to dissociate into dimers upon dilution from micromolar to nanomolar con-

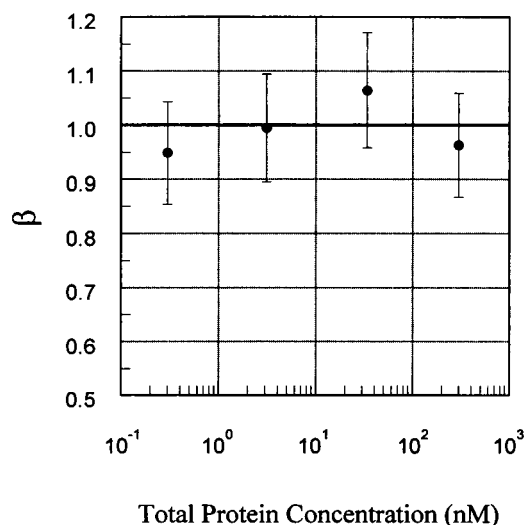


FIGURE 5 Particle number measured for multiple concentrations of B phycoerythrin. The quantity β was defined in Eq. 2. A value of 1 corresponds to one measured particle per nominal molecule. As shown, this protein does not change oligomeric states as it is diluted over the measured concentration range.

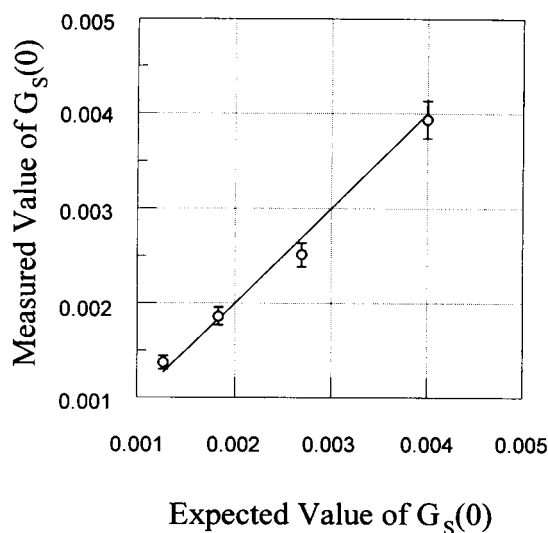


FIGURE 6 Mixtures of 7-nm (small) and 15-nm (large) radius spheres. The expected values of $G_S(\tau)$ are calculated using the known relative intensities and relative concentrations of the two sizes. The average number of spheres in the excited volume are \bullet , 115 small, 0.85 large; \blacksquare , 108 small, 1.7 large; \square , 97 small, 3.3 large; \circ , 59 small, 4.2 large.

centrations (Huang and Graves, 1970; Wang and Graves, 1964; Ruan and Weber, 1993). Fig. 7 shows a typical measurement of $G_S(\tau)$ for 8 nM GPA. Although the signal-to-noise ratio remains reasonably high, the noise is clearly more significant for these dimmer samples. It was necessary to average each data point taken between 15 and 30 min. Measurements were repeated several times at each of eight separate protein concentrations, and the results were averaged. The reproducibility of repeated measurements was 5–10%. The results from a series of protein concentrations are shown in Fig. 8. The curve represents the least-squares

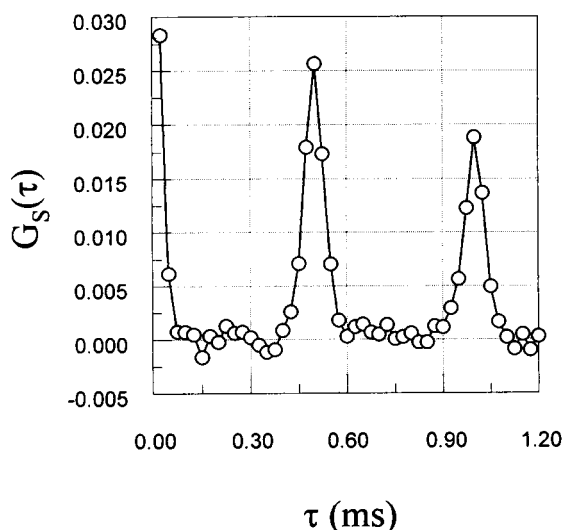


FIGURE 7 A typical measurement of $G_S(\tau)$ for glycogen phosphorylase A with a 2-kHz scanning rate. The protein concentration was 8 nM.

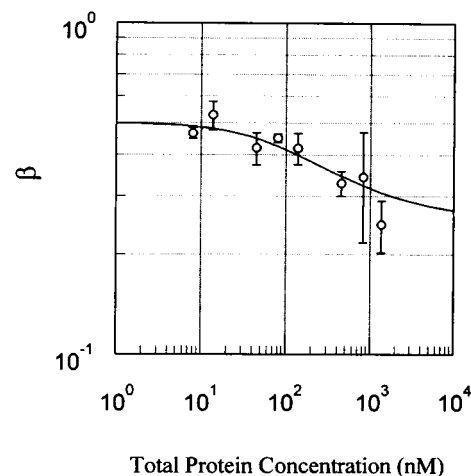


FIGURE 8 The dissociation of GPA as it is diluted from micromolar to nanomolar concentration. The curve represents the best fit to Eq. 3. A value of 0.25 corresponds to a factor of four fewer molecules than the nominal value, and 0.5 to a factor of two fewer than the nominal value, corresponding to tetramer and dimer populations, respectively. The concentration at which $\beta = 0.33$ corresponds to the dissociation constant.

fit using Eq. 3, assuming an equilibrium population of dimers and tetramers only. The fit yields a value of $K_d = 430$ nM (monomer), in good agreement with the previously published values (Huang and Graves, 1970; Ruan and Weber, 1993).

A similar data set was acquired with MDH, as shown in Fig. 9. This protein was a more difficult test because of the faster diffusion rates of this smaller protein. The 2-kHz scan rate used is the maximum attainable rate for the current instrument. Data shown are again average values from repeated measurements at each protein concentration. These data were fit in the same manner as above with $K_d = 144$

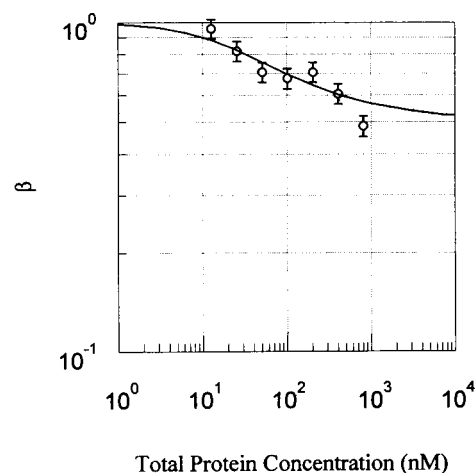


FIGURE 9 The dissociation of MDH as the protein concentration is diluted. Measurements were made with a 2-kHz scanning rate. A value of 1 corresponds to the monomer, 0.5 to the dimer, and the concentration at which $\beta = 0.66$ is the value of the dissociation constant.

nM, again in reasonable agreement with previously reported values (D. Jameson, personal communication; Shore and Chakrabarti, 1976). The dissociation constant of MDH is known to vary, depending on methods of sample preparation (D. Jameson, personal communication). Further investigation of this phenomenon can be an interesting future application of scanning FCS.

Two final sets of experiments were performed using rabbit muscle PFK, first to measure the kinetics of dissociation after dilution, and then to monitor dissociation upon titration to acidic pH (after equilibration). The stock PFK sample (3.9 mM, pH 7.5) was diluted to 100 nM at pH 8.0. $G_S(T)$ was measured repeatedly over several hours. At the initial concentration, the protein is mostly tetramers and larger aggregates. Upon dilution to 100 nM, the protein dissociates to a distribution of dimers and tetramers. Fig. 10 shows the time course of the dissociation, which was fit to an exponential relaxation with a time constant of 0.15 h. The time scale is consistent with previous measurements (Lad et al., 1976). Although more measurements are clearly needed to make any conclusions about the kinetic behavior, these data suggest interesting possibilities for future experiments. Each data point in this set was averaged for 20 min. This long data acquisition time was necessary mostly because of the low fluorescent yield of the BODIPY label. In contrast, the sphere measurements discussed above can currently be made on the time scale of seconds. Planned optical improvements to the instrument, in conjunction with brighter probes, can make kinetic measurements of protein interactions possible on this time scale as well.

Finally, Fig. 11 shows the dissociation of 100 nanomolar PFK upon titration from pH 8.5 to pH 5.0. The $G_S(T)$ values show that the protein does dissociate to some degree between these pH values. This transition to a more dissociated form between pH 7.0 and pH 6.0 agrees reasonably well with previous reports of this phenomenon using ultracentrifugation (Aaronson and Frieden, 1972; Pavelich and

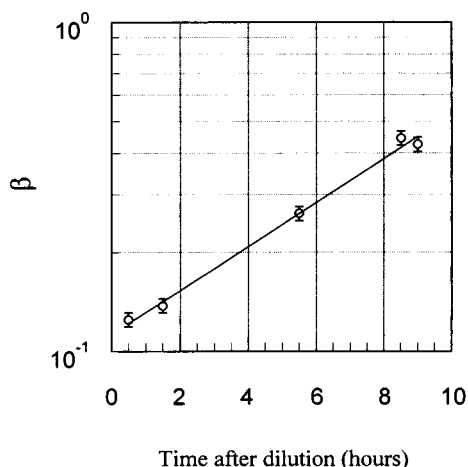


FIGURE 10 Kinetic measurements of the dissociation of PFK after diluting from 3.9 μ M to 100 nM. Each measurement (data point) was averaged for 20 min.

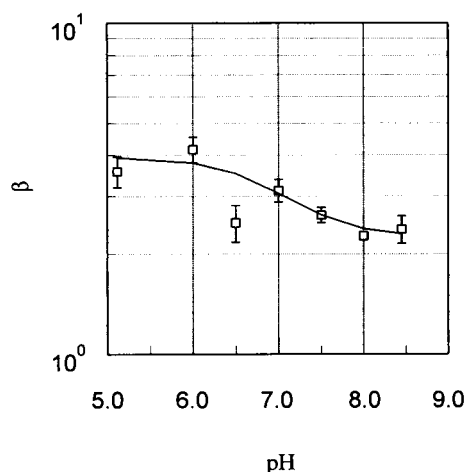


FIGURE 11 The dissociation of phosphofructokinase with pH.

Hammes, 1973). At the measured enzyme concentration, the protein is already partly dissociated to dimer form (Pavelich and Hammes, 1973), and thus the $G_S(T)$ transition does not undergo a full tetramer-dimer transition as pH is altered. We experienced some difficulty with the pH 6.5 sample, with lower reproducibility of repeated measurements than normally observed for this instrument. We suspect that the presence of some unstable aggregates may cause this observation. Other studies of PFK in this pH range have found similar effects (Aaronson and Frieden, 1972).

DISCUSSION

We have shown particle-counting measurements over four orders of magnitude in concentration. This capability was demonstrated first with multiple concentrations of 7-nm and 15-nm latex beads, and then with B phycoerythrin. The smaller beads are close in size to many relatively large proteins, such that results for these samples should be reasonably characteristic of the instrument's capability to measure other small particles, with comparable fluorescence intensity. In test measurements not shown in this report, fluorescence intensity from the 7-nm spheres was attenuated to the level of GPA samples (of the same number concentration) using emission filters. Although more time was required to achieve the same signal-to-noise ratio, the results still proved quite accurate. For clean monodisperse samples, scanning FCS functions very well for fast, accurate particle counting. Typical measurements with the small spheres can be completed in under 10 s.

$G_S(T)$ values were also measured for mixtures of 7-nm and 15-nm spheres. With the assumption that the samples contained only two species of known relative intensity, the measured distribution reproduced the known sample composition reasonably well. The current procedure is sufficient for samples containing only two species with known relative intensity. For more complicated distributions of particle

sizes, more information is needed to uniquely determine sample composition. However, even in these cases one can still detect aggregation or other changes in sample composition, although complete particle size distributions may not be recovered.

The scanning FCS application proposed and demonstrated in this work is the detection of the association/dissociation equilibria of protein oligomers. Examples of dissociation as concentration was diluted were shown for glycogen phosphorylase A (dimer-tetramer), malate dehydrogenase (monomer-dimer), and phosphofructokinase (dimer-tetramer/*n*-mer). All of the measured dissociation constants are reasonably consistent with previously reported values, although higher resolution binding curves are the ultimate goal. Using this method, it is possible to perform similar studies on other proteins. The present data quality suggests that other methods, such as fluorescence polarization, are preferred in some cases. However, FCS measurements are independent of molecular rotational rates, because of the counting nature of these experiments. Thus, scanning FCS can monitor association for large molecules, or for environments where molecular rotational rates are too slow (or obscured by local probe motions) to gain information from polarization. In such cases, scanning FCS provides information that is otherwise difficult to obtain. Furthermore, applications of scanning FCS can be easily generalized beyond protein-protein interactions. FCS can be used to study many other interesting biochemical phenomena, such as how the subunit composition of an enzyme varies as ligands are added or removed, or interactions of DNA binding proteins with nucleic acids. It should also be possible to apply this method to the study of membrane-bound molecules, including receptor aggregation.

In addition to measuring aggregation at multiple protein concentrations, alternative experiments may vary other parameters, such as pressure, salt concentration, pH, or presence/concentration of ligand. The dissociation of PFK upon titration from pH 8 to pH 5 is presented as an example. Also shown with the PFK is the possibility of measuring kinetics. Although current data acquisition times are suitable only for relatively slow reactions, planned improvements discussed below should make faster data acquisition times possible.

Again, the main requirement for a successful experimental application of FCS is the ability to accurately measure the number of particles in the excited volume. The number of fluorescence photons detected per particle in the volume per sampling time is the key parameter (Koppel, 1974; Brenner et al., 1978). Also important is a low background level, because high dark counts and scattered light can distort values recovered from the fluctuation statistics. Two-photon excitation is particularly useful for low noise detection, as discussed above. When "per particle" counting rates and overall light levels are high, FCS measurements are fast and accurate, as in the sphere measurements shown above. Data collection times increase quickly as light levels diminish. However, the labeling of two FITCs per monomer used in these studies was sufficient. It should also be possible to

do experiments with only a single chromophore per monomer. We have demonstrated single chromophore sensitivity with this instrument (Berland et al., 1996).

There are limits to the range of sample concentrations that can be measured using FCS. As concentration in increased, fluctuation amplitudes decrease. The upper concentration limit is reached when instrument noise becomes larger than the amplitude of occupation number fluctuations, typically around 1 to 10 μM (i.e., 100 to 1000 particles per volume sampled). There are several factors that contribute to the lower limit on measurable concentrations. First, the presence of impurities can be a major limitation, and if contaminants are in the buffers used to dilute samples, their concentration remains fixed while the real sample signal is decreased. Furthermore, at low concentrations, there are fewer fluctuation "events", which can lead to prohibitively long data acquisition times. The lowest measured concentration reported in this article was 0.2 nM, for 15-nm spheres. This value was a convenient stopping point, although it is not an actual limit. Lower concentrations are accessible, although at the expense of data collection time. In other words, when particle occupation numbers become extremely low ($\ll 1$), it can take too long for particles to reach the excited volume, even if they are easily detected once in the volume. For these concentrations, particle-counting applications may or may not be practical, but FCS analysis can still be used to identify and characterize the presence and diffusion rates of certain molecular species (Eigen and Rigler, 1994). It may be possible to decrease the event time for dilute concentrations by using a directed flow of particles, as in capillary electrophoresis.

Another way to extend the lower concentration limit is to increase the size of the volume, thus keeping the average occupation number higher. A larger excitation volume can be obtained by using a diaphragm before the objective lens. A larger volume will also increase the diffusion turnover time discussed above, which can be advantageous for rapidly diffusing molecules. Longer crossing times, however, may also cause photochemical destruction (bleaching) of chromophores, which can become an important concern. Another disadvantage is that larger volumes would necessitate larger scanning radii. As the scan radius is increased, it becomes difficult to achieve a uniform volume size and constant fluorescence collection efficiency for all points in the scanning path (scanning the sample can avoid this). Still, if lower concentrations are of particular interest, a larger excited volume can help make the FCS measurements more practical.

The diffusion coefficient of sample particles is also an important factor in determining which samples and concentration ranges can be measured. Faster diffusing particles necessitate faster scanning, and consequently higher sampling rates to measure $G_s(\tau)$. The consequence is less time to sample any given subvolume, which results in fewer counts per particle per sampling time and longer data acquisition. Using high-viscosity solvents or a larger excita-

tion volume will slow down diffusion and can help avoid this limitation.

The major improvements that can be made in the current instrument are in the light collection efficiency and data analysis procedures. The microscope used is not designed for single particle detection. The current light collection efficiency ($\sim 0.1\%$) can be improved significantly with some adjustments to the optical path, including the elimination of several unnecessary lenses and windows. We have designed and are constructing a new microscope for this purpose. In addition, although the current photomultiplier tube is very good for low noise detection, the higher quantum efficiency of an avalanche photodiode would be an improvement for very dim samples. We currently anticipate an increase in overall detection efficiency of ~ 5 – 10 times. This will be a major advance because the correlated signal depends on the square of the signal amplitude. At these higher light collection levels, protein samples used in this work would have a fluorescence intensity equivalent to the current brightness of the latex spheres. A second important improvement that can be made to the current procedure is in the data analysis. Fitting the peak shapes, the series of peaks, or both should be a major improvement over the current, single-point procedure. Furthermore, a more sophisticated analysis, perhaps including higher order correlation, may result in the ability to fully recover the distribution of particle sizes, further enhancing the measurement resolution.

The high sensitivity, selectivity, and low background levels of two-photon excitation are ideal for applications of scanning FCS. The instrument provides accurate quantitative information about particle number concentrations, as demonstrated using latex spheres of size and intensity comparable to the biomolecules studied. We have shown that these particle number measurements can be used to detect molecular associations in solution at equilibrium. The method was used to monitor protein interactions at low concentrations. Combined with FCS measurements of diffusion, the method can be a powerful diagnostic tool. The potential to monitor association kinetics has also been demonstrated. Current single-point measurements have been made in tens of seconds for latex spheres and in 5–20 min for protein samples. This time scale is sufficient to study many protein association/dissociation reactions. FCS is most useful at low concentrations ($< \mu\text{M}$), where other techniques become difficult, and thus complements these other methods well. We envision that the proposed improvements in the instrument will enhance the overall resolution of this technique and reduce data acquisition times, leading to greater time resolution for kinetic measurements. Two-photon scanning FCS is a promising, powerful new technique for studying molecular associations and interactions.

We wish to thank D. Jameson and G. Reinhart for their assistance with MDH and PFK, respectively.

This work was supported by the National Institutes of Health (RR03155).

REFERENCES

- Aaronson, R. P., and C. Frieden. 1972. Rabbit muscle phosphofructokinase: studies on the polymerization—the behavior of the enzyme at pH 8, pH 6, and intermediate pH values. *J. Biol. Chem.* 47:7502–7509.
- Berland, K. M., P. T. C. So, and E. Gratton. 1995. Two-photon fluorescence correlation spectroscopy: method and application to the intracellular environment. *Biophys. J.* 68:694–701.
- Berland, K. M., P. T. C. So, T. Ragan, W. Yu, and E. Gratton. 1996. Two-photon excitation for low background fluorescence microscopy: detection of single molecules and single chromophores in solution. *Biophys. J.* 70:A429.
- Brenner, S. L., R. J. Nossal, and G. H. Weiss. 1978. Number fluctuation analysis of random locomotion statistics of a Smoluchowski process. *J. Stat. Phys.* 18:1–18.
- Denk, W., J. H. Strickler, and W. W. Webb. 1990. Two-photon laser scanning fluorescence microscopy. *Science*. 248:73–76.
- Eigen, M., and R. Rigler. 1994. Sorting single molecules: application to diagnostics and evolutionary biotechnology. *Proc. Natl. Acad. Sci. USA*. 91:5740–5747.
- Elson, E. L., and D. Magde. 1974. Fluorescence correlation spectroscopy. I. Conceptual basis and theory. *Biopolymers*. 13:1–27.
- Huang, Y. C., and D. J. Graves. 1970. Correlation between subunit interactions and enzymatic activity of phosphorylase a. Method for determining equilibrium constants from initial rate measurements. *Biochemistry*. 9:660–671.
- Huang, Z., and N. L. Thompson. 1996. Imaging fluorescence correlation spectroscopy: nonuniform IgE distributions on planar membranes. *Biophys. J.* 70:2001–2007.
- Icenogle, R. D., and E. L. Elson. 1983. Fluorescence correlation spectroscopy and photobleaching recovery of multiple binding reactions. II. FPR and FCS measurements at low and high DNA concentrations. *Biopolymers*. 22:1919–1948.
- Koppel, D. E. 1974. Statistical accuracy in fluorescence correlation spectroscopy. *Phys. Rev. A*. 10:1938–1945.
- Koppel, D. E., F. Morgan, A. Cowan, and J. H. Carson. 1994. Scanning concentration correlation spectroscopy using the confocal laser microscope. *Biophys. J.* 66:502–507.
- Lad, P. M., D. E. Hill, and G. G. Hammes. 1976. Influence of allosteric ligands on the activity and aggregation of rabbit muscle phosphofructokinase. *Biochemistry*. 12:4303–4309.
- Magde, D., E. L. Elson, and W. W. Webb. 1974. Fluorescence correlation spectroscopy. II. An experimental realization. *Biopolymers*. 13:29–61.
- Mertz, J., C. Xu, and W. W. Webb. 1995. Single-molecule detection by two-photon-excited fluorescence. *Optics Lett.* 20:2532–2534.
- Mets, U., and R. Rigler. 1994. Submillisecond detection of single rhodamine molecules in water. *J. Fluorescence*. 4:259–264.
- Meyer, T., and H. Schindler. 1988. Particle counting by fluorescence correlation spectroscopy: simultaneous measurement of aggregation and diffusion of molecules in solution and in membranes. *Biophys. J.* 54:983–993.
- Palmer, A. G., and N. L. Thompson. 1987. Molecular aggregation characterized by high order autocorrelation in fluorescence correlation spectroscopy. *Biophys. J.* 52:257–270.
- Palmer, A. G., and N. L. Thompson. 1989a. Intensity dependence of high-order autocorrelation functions in fluorescence correlation spectroscopy. *Rev. Sci. Instrum.* 60:624–633.
- Palmer, A. G., and N. L. Thompson. 1989b. Fluorescence correlation spectroscopy for detecting submicroscopic clusters of fluorescent molecules in membranes. *Chem. Phys. Lipids*. 50:253–270.
- Pavelich, M. J., and G. Hammes. 1973. Aggregation of rabbit muscle phosphofructokinase. *Biochemistry*. 12:1408–1414.
- Petersen, N. O. 1984. Diffusion and aggregation in biological membranes. *Can. J. Biochem. Cell Biol.* 62:1158–1166.
- Petersen, N. O. 1986. Scanning fluorescence correlation spectroscopy. I. Theory and simulation of aggregation measurements. *Biophys. J.* 49:809–815.
- Petersen, N. O., P. L. Hoddellius, P. W. Wiseman, O. Seger, and K. E. Magnusson. 1993. Quantitation of membrane receptor distributions by

- image correlation spectroscopy: concept and application. *Biophys. J.* 65:1135–1146.
- Petersen, N. O., D. C. Johnson, and M. J. Schlesinger. 1986. Scanning fluorescence correlation spectroscopy. II. Application to virus glycoprotein aggregation. *Biophys. J.* 49:809–815.
- Qian, H., and E. L. Elson. 1990a. On the analysis of high order moments of fluorescence fluctuations. *Biophys. J.* 57:375–380.
- Qian, H., and E. L. Elson. 1990b. Distribution of molecular aggregation by analysis of fluctuation moments. *Proc. Natl. Acad. Sci. USA.* 87: 5479–5483.
- Ragan, T., K. M. Berland, P. T. C. So, M. Yu, and E. Gratton. 1996. Imaging a single fluorophore using two-photon excitation. *Biophys. J.* 70:429a.
- Rigler, R., U. Mets, J. Widengren, and P. Kask. 1993. Fluorescence correlation spectroscopy with high count rate and low background: analysis of translational diffusion. *Eur. Biophys. J.* 22:169–175.
- Rigler, R., J. Widengren, and U. Mets. 1992. Interactions and kinetics of single molecules as observed by fluorescence correlation spectroscopy. In *Fluorescence Spectroscopy. New Methods and Applications*. I. S. Wolfbeis, editor. Springer, New York. 13–24.
- Ruan, K., and G. Weber. 1993. Physical heterogeneity of muscle glycogen phosphorylase revealed by hydrostatic pressure dissociation. *Biochemistry.* 32:6295–6301.
- Shore, J. D., and S. K. Chakrabarti. 1976. Subunit dissociation of mitochondrial malate dehydrogenase. *Biochemistry.* 15:875–879.
- St-Pierre, P. R., and N. O. Petersen. 1990. Relative ligand binding to small or large aggregates measured by scanning correlation spectroscopy. *Biophys. J.* 58:503–511.
- Thompson, N. L. 1991. Fluorescence correlation spectroscopy. In *Topics in Fluorescence Spectroscopy*. Vol. 1. Techniques. J. R. Lakowicz, editor. Plenum, New York. 337–378.
- Wang, J. H., and D. Graves. 1964. The relationship of the dissociation to the catalytic activity of glycogen phosphorylase a. *Biochemistry.* 3:10, 1437–1445.
- Weissman, M., H. Schindler, and G. Feher. 1976. Determination of molecular weights by fluctuation spectroscopy: application to DNA. *Proc. Natl. Acad. Sci. USA.* 73:2776–2780.
- Widengren, J., R. Rigler, and U. Mets. 1994. Triplet-state monitoring by fluorescence correlation spectroscopy. *J. Fluorescence.* 4:255–258.